ADVANCES IN ATMOSPHERIC SCIENCES, VOL. 24, NO. 2, 2007, 323–335

Improvements in Climate Simulation with Modifications to the Tiedtke Convective Parameterization in the Grid-Point Atmospheric Model of IAP LASG (GAMIL)

LI Lijuan[1,3] (李立娟), WANG Bin*[1] (王 斌), Yuqing WANG[2], and Hui WAN[1,3]

[1] *State Key Laboratory of Numerical Modeling for Atmospheric Sciences and Geophysical Fluid Dynamics, Institute of Atmospheric Physics, Chinese Academy of Sciences, Beijing* 100029

[2] *Department of Meteorology and International Pacific Research Center, University of Hawaii at Manoa, Honolulu, HI* 96822

[3] *Graduate University of the Chinese Academy of Sciences, Beijing* 100039

(Received 7 March 2006; revised 14 July 2006)

ABSTRACT

The grid-point atmospheric model of IAP LASG (GAMIL) was developed in and has been evaluated since early 2004. Although the model shows its ability in simulating the global climate, it suffers from some problems in simulating precipitation in the tropics. These biases seem to result mainly from the treatment of the subgrid scale convection, which is parameterized with Tiedtke's massflux scheme (or the Zhang-McFarlane scheme, as an option) in the model. In order to reduce the systematic biases, several modifications were made to the Tiedtke scheme used in GAMIL, including (1) an increase in lateral convective entrainment/detrainment rate for shallow convection, (2) inclusion of a relative humidity threshold for the triggering of deep convection, and (3) a reduced efficiency for the conversion of cloud water to rainwater in the convection scheme.

Two experiments, one with the original Tiedtke scheme used in GAMIL and the other with the modified scheme, were conducted to evaluate the performance of the modified scheme in this study. The results show that both the climatological mean state, such as precipitation, temperature and specific humidity, and interannual variability in the model simulation are improved with the use of this modified scheme. Results from several additional experiments show that the improvements in the model performance in different regions mainly result from either the introduction of the relative humidity threshold for triggering of the deep convection or the suppressed shallow convection due to enhanced lateral convective entrainment/detrainment rates.

Key words: GAMIL, Tiedtke convection scheme, double ITCZ, RH threshold

DOI: 10.1007/s00376-007-0323-3

1. Introduction

GAMIL is a grid-point atmospheric general circulation model (GCM) developed in the State Key Laboratory for Numerical Modeling for Atmospheric Sciences and Geophysical Fluid Dynamics (LASG), Institute of Atmospheric Physics (IAP), Chinese Academy of Sciences (CAS). The model uses the dynamical core developed by Wang et al. (2004a) and the physics package of the Community Atmospheric Model Version 2 (CAM2) of the National Center for Atmospheric Research (NCAR) (Collins et al., 2003).

The model equations are solved on a hybrid horizontal grid with the Gaussian grid in the region between 65.58°S and 65.58°N (the resolution was 2.8° × 2.8°) and with a weighted even area grid in the high latitudes and polar region. The model has 26 vertical levels in σ (pressure normalized by surface pressure) coordinate, with the model top at 2.194 hPa, where a solid lid boundary condition is applied. Because of the use of this weighted even-area grid system in the high latitudes and polar regions, the new dynamical core

*E-mail: wab@lasg.iap.ac.cn

of Wang et al. (2004a) is computationally quite stable and therefore neither filtering nor smoothing is applied to the model even in the polar regions. Most especially, some important integral properties are maintained[a], such as the anti-symmetries of the horizontal advection operator and the vertical advection operator, the mass conservation, the effective total energy conservation under the standard stratification approximation (Wang et al., 2004a).

The model physics include cloud and precipitation processes, radiation, land surface and sea ice modules, and turbulent mixing. Two massflux convection schemes are included and can be chosen optionally: the Tiedtke scheme (1989) modified by Nordeng (1994) from ECHAM (Roeckner et al., 1996) and the Zhang and McFarlane (1995) scheme from the original NCAR CAM2. The two-step shape-preserving advection scheme developed by Yu (1994) is utilized for the time integration of the water vapor mixing ratio equation.

GAMIL, with the use of the Tiedtke scheme modified by Nordeng (1994), is able to simulate many observed climatological features. In particular, the model with the Zhang-McFarlane convective scheme produces spurious heavy rainfall over the south and southeast slopes of the Tibetan Plateau in boreal summer[b], which is eliminated with the use of the Tiedtke scheme. Nevertheless, there are still several significant discrepancies in the model mean climate simulation of precipitation, the vertical structure of the atmosphere, and the interannual variability. An obvious double-ITCZ (Intertropical convergence zone) phenomenon appears in the western-central Pacific and a break in ITCZ precipitation appears in the central-eastern Pacific in boreal summer, which is a common problem in the atmospheric GCM as well as the coupled GCM (Mechoso et al., 1995; Zhang and Wang, 2006). Precipitation in the South Pacific Convergence Zone (SPCZ) is underestimated, but overestimated over South America and South Africa in boreal winter. The zonal mean precipitation in the tropics is generally underestimated compared to observations[b]. We will show in this study that several modifications to the Tiedtke convection scheme can considerably improve the model simulations.

The remainder of this paper is organized as follows. Section 2 describes the modifications to the convection scheme, the experimental design, and the data used in verification of the model simulations. The simulation results, including the climatological mean, interannual variability and the effects of the individual changes to the convection scheme are discussed in section 3. The main conclusions are drawn in the last section.

2. Modifications to the convection scheme and experimental design

2.1 *Modifications to the Tiedtke convection scheme*

The Tiedtke (1989) convective parameterization scheme is based on the mass flux concept and a bulk cloud model. The scheme considers three types of convection. The first type is deep convection under disturbed, conditionally unstable conditions in the presence of lower tropospheric large-scale moisture convergence. The second is shallow convection under undisturbed conditions and is mainly driven by the turbulent surface moisture flux. The third type is the so-called mid-level convection that occurs mainly in conditionally unstable situations but with a cloud base well above the planetary boundary layer. Only one type of convection is allowed to take place in a grid box during each time step. An ensemble of clouds occurring in each type of convection is assumed to consist of updrafts and downdrafts. Updrafts are allowed to interact with the environment through convective entrainment and detrainment. Both the lateral entrainment/detrainment due to turbulence and the organized entrainment/detrainment due to organized inflow/outflow near the cloud base/top are considered following certain assumptions and simplifications. Downdrafts are assumed to occur at the level of free sinking (LFS), where in-cloud air mixes with environmental air and becomes unstable in relation to the surrounding environment. The mass flux at LFS is taken as 30% of the cloud-base mass flux (Tiedtke, 1989).

Nordeng (1994) introduced a new closure assumption for deep convection within the original Tiedtke scheme. In the modified scheme by Nordeng, the mass flux at the cloud base is determined by the convective available potential energy (CAPE) instead of the original moisture convergence closure. He also assumed that the organized entrainment takes place if buoyancy is present locally, i.e., entrainment is related to the activity of the cloud itself. The connection to local buoyancy leads to weaker mass flux at the cloud base

[a]B. Wang, and Coauthors, 2006: A new grid-point AGCM using a semi-implicit scheme with exact quadratic conservation, Part 1: Dynamical Core, to be submitted.

[b]H. Wan, and Co-authors, 2006: A new grid-point AGCM using a semi-implicit scheme with exact quadratic conservation, Part 2: Climatology Simulations from the AMIP II Experiment, to be submitted.

H. Wan, and Coauthors, 2006: Development and Validation of the Gridpoint Atmospheric Model of IAP LASG (GAMIL), LASG Technical Report No. 16, 84pp.

Table 1. Summary of numerical experiments.

Experiments	Comments
CNTRL	The original Tiedtke convection scheme in GAMIL
SENS1	With the three modifications to the original Tiedtke scheme as outlined in section 2a
SENS2	As in SENS1, but with the 80% RH threshold removed
SENS3	As in CNTRL, but with the suppressed shallow convection included

but higher values of entrainment in comparison to the connections with the large-scale circulation used in the original Tiedtke scheme (Dümenil and Bauer, 1998).

Here, based on the results of Wang et al. (2003, 2004b), Wang et al. (2004c) and Wang et al. (2006), we have made three modifications to the Tiedtke scheme used in GAMIL to improve the simulation of tropical precipitation. First, the average fractional lateral entrainment/detrainment rate for shallow convection is increased from the original 3×10^{-4} m^{-1} to 2×10^{-3} m^{-1}, a value close to that inferred from the large-eddy simulation results of Siebesma and Holtslag (1996). Note that although shallow convection involves non-precipitating clouds, it plays an important role in heat and moisture transport in the lower troposphere. The larger lateral entrainment/detrainment rate is used to limit the overly active shallow convection. Secondly, a relative humidity threshold of 80% in the environment is imposed on the detected cloud column as the triggering for deep convection thus avoiding the occurrence of convection under relatively dry conditions. A similar relative humidity threshold has also been included in the Zhang-McFarlane convection parameterization used in CCM3 (Zhang and McFarlane, 1995). Thirdly, the conversion coefficient of cloud water to rain water in the convection scheme was reduced from 6×10^{-3} s^{-1} to 2×10^{-3} s^{-1}. This was modified to limit the efficiency of hydrological cycle for convective precipitation.

2.2 *Experimental design and observational data*

Four experiments were performed using GAMIL using both the original and modified convective schemes (Table 1). In the first experiment (CNTRL), the original settings in the GAMIL Tiedtke scheme were used. In the second experiment (SENS1), all modifications to the convection scheme described in section 2.1 were instituted into GAMIL. In the third experiment (SENS2), the relative humidity threshold for deep convection triggering was removed and in the last experiment (SENS3), only the modification to shallow convection was included. The last two experiments were designed to examine which improvements made to the Tiedtke scheme provided the best modeling of observables.

The simulations described here were conducted following the standard settings for the Atmospheric Model Intercomparision Project (AMIP) II experiments with the solar constant, the orbital parameters and CO_2 concentration set to those of the current climate. The lower boundary conditions of the model atmosphere are the sea surface temperature (SST) and sea ice from the Program for Climate Model Diagnosis and Intercomparison (PCMDI) (Phillips, 1996) interpolated into the model grids. Each experiment was run for 20 years, encompassing the time frame of 1 January 1979 to 31 December 1998. Monthly mean outputs are interpolated onto 17 pressure levels similar to those in the verification data.

The monthly mean data used for verification of model simulations are those provided by the National Centers for Environmental Prediction/ Department of Energy AMIP II Reanalysis (often referred to as NCEP/DOE Reanalysis) (Kanamitsu et al., 2002). The monthly mean precipitation rate is the Climate Prediction Center's Merged Analysis of Precipitation (CMAP; Xie and Arkin, 1997). Both datasets are at $2.5^\circ \times 2.5^\circ$ resolution in the horizontal. In order to compare with the observations, the model outputs are interpolated into the same grid system as in observations. Note that the first year model results were regarded as model spin-up and thus excluded from the analysis below.

3. Results

3.1 *Climatological mean*

Figure 1 displays the distribution of the 19-year mean precipitation for boreal winter (December, January, and February, DJF) obtained from the observations and results from the CNTRL and SENS1 runs. Overall the model simulated the distribution of precipitation reasonably well under both the CNTRL and SENS1 tests, but the latter was superior in several details. In the control run (Fig. 1c), there are two precipitation maxima in the Maritime Continent and western Pacific warm pool region on each side of the equator, a phenomenon called "double ITCZ". The ITCZ north of the equator is too strong, while the south one is too weak compared to the observations

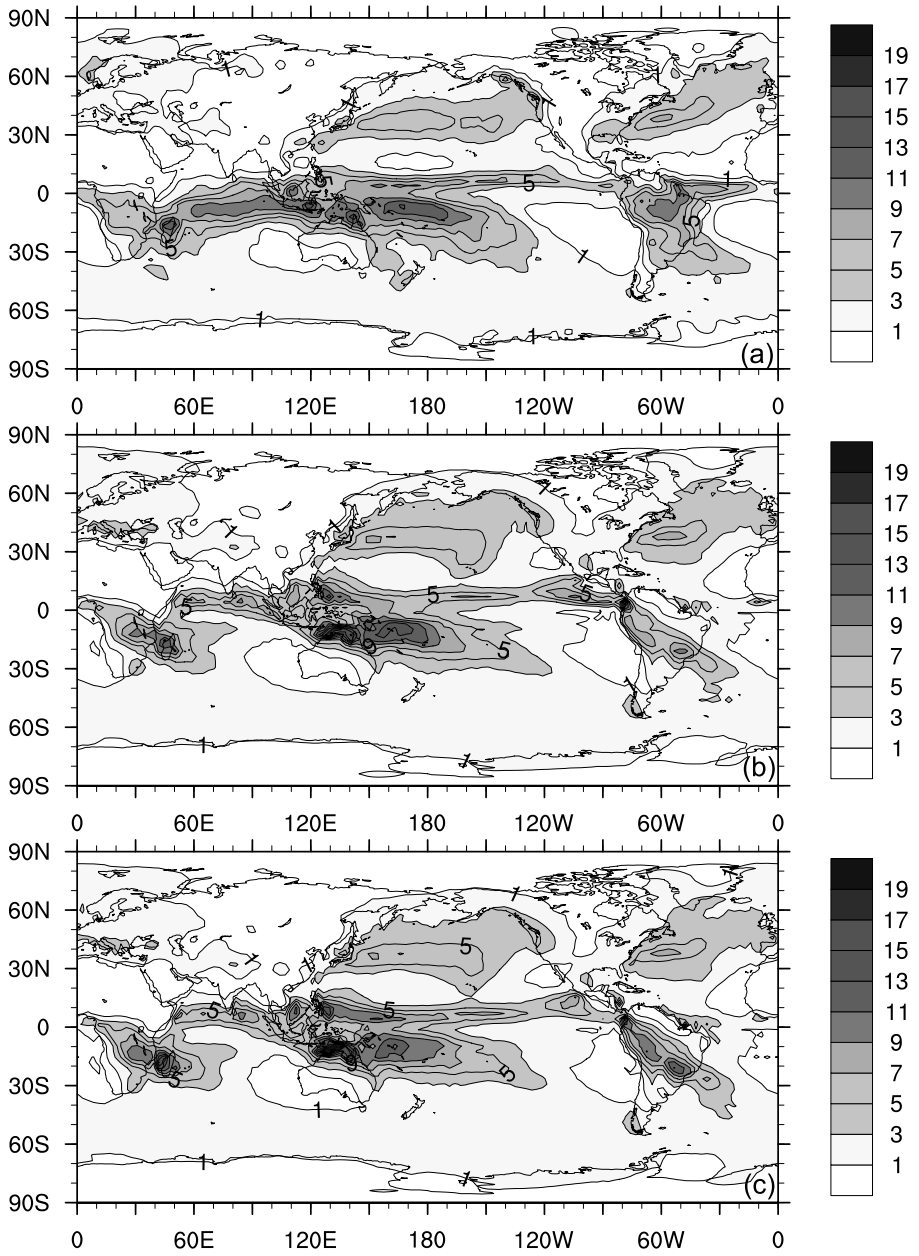

Fig. 1. Long-term mean precipitation (mm d^{-1}) in boreal winter (DJF) (a) from CMAP and from model simulations (b) SENS1 and (c) CNTRL run.

(Fig. 1a). The rainfall was considerably overestimated over central South America, South Africa, and Madagascar, underestimated in the South Pacific Convergence Zone (SPCZ). In experiment SENS1, the rainfall maximum to the north of the equator in the western Pacific warm pool region is significantly reduced, and rainfall amount over the central South America, South Africa and Madagascar is largely reduced, while it was increased in the SPCZ, therefore providing simulations that were closer to the observations (Fig. 1b). Therefore, GAMIL, when the modifications to the Tiedtke convection scheme were included, saw improvements in the simulation of boreal winter precipitation compared to the results of the same model with the original Tiedtke convection scheme.

Figure 2 shows the distribution of the 19-year mean precipitation in boreal summer (JJA). There were three severe discrepancies in the simulated precipitation from CNTRL: a too strong double ITCZ in the Maritime Continent and the western Pacific warm pool region, similar to that for boreal winter, a break in the simulated precipitation in the ITCZ region north

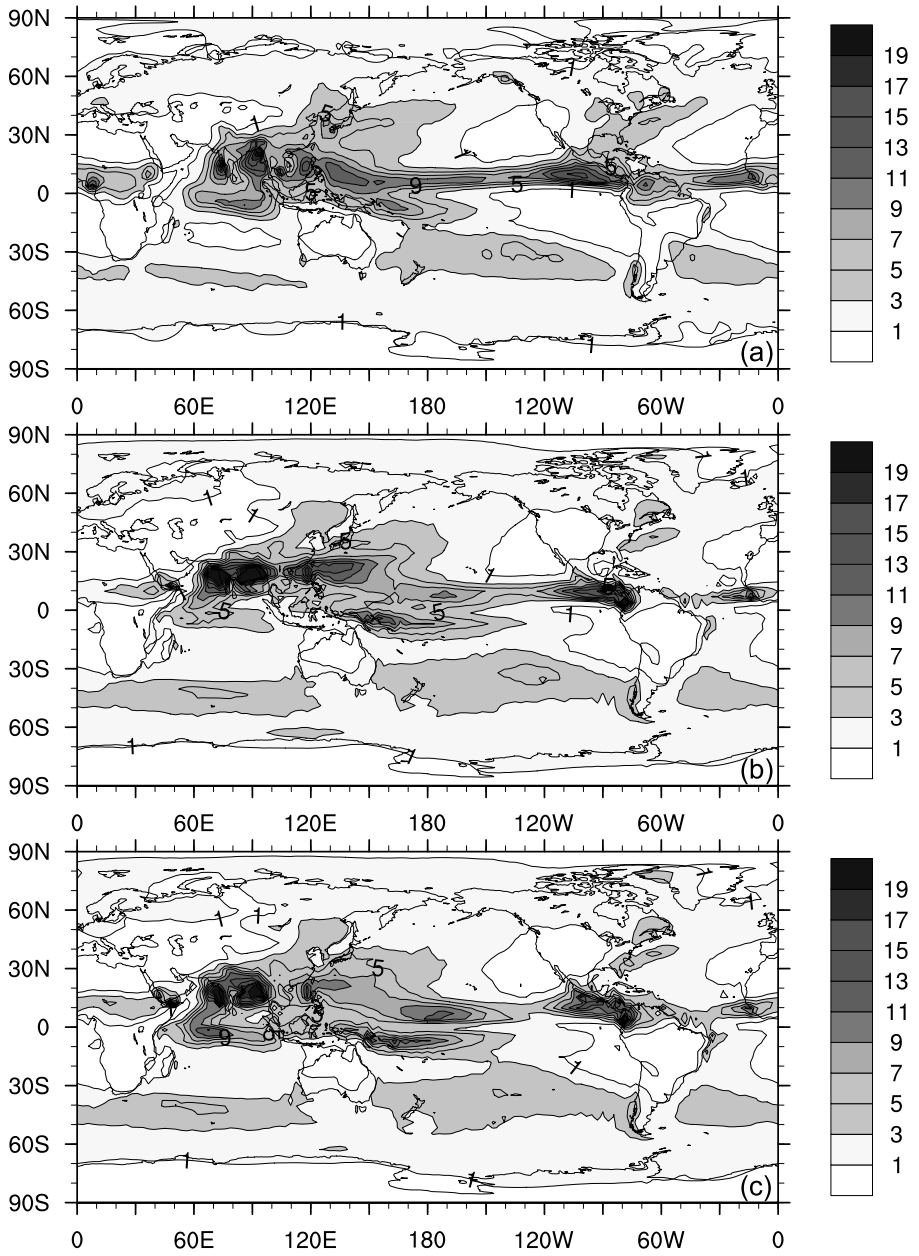

Fig. 2. The same as in Fig. 1 but for boreal summer (JJA).

of the equator in the central-eastern Pacific and a considerable underestimation of the precipitation in the tropical western North Pacific. Furthermore, an overestimation of the precipitation was found in the ITCZ region north of the equator around the dateline (Fig. 2c). These discrepancies were remarkably eliminated in the experiment SENS1 (Fig. 2b). Now the "double ITCZ" is not as prevalent as in the CNTRL simulation and the break in ITCZ precipitation over the central-eastern Pacific no longer exists (Fig. 2b). Precipitation over the western North Pacific warm pool region is increased and is therefore closer to the observations (Figs. 2a, b). In addition, precipitation in the SPCZ is better simulated via the SENS1 test than by the CNTRL method, although the SENS1 simulation did produce a shift to the east in precipitation maximum. This improvement can be mainly attributed to the improvement in the simulation of grid-resolved stratiform precipitation (not shown). However both experiments underestimated the precipitation in the Atlantic ITCZ and in tropical Africa. SENS1 also considerably underestimated the precipitation in the Northern part of South America (Fig. 2b).

A realistic simulation of fractions of large-scale

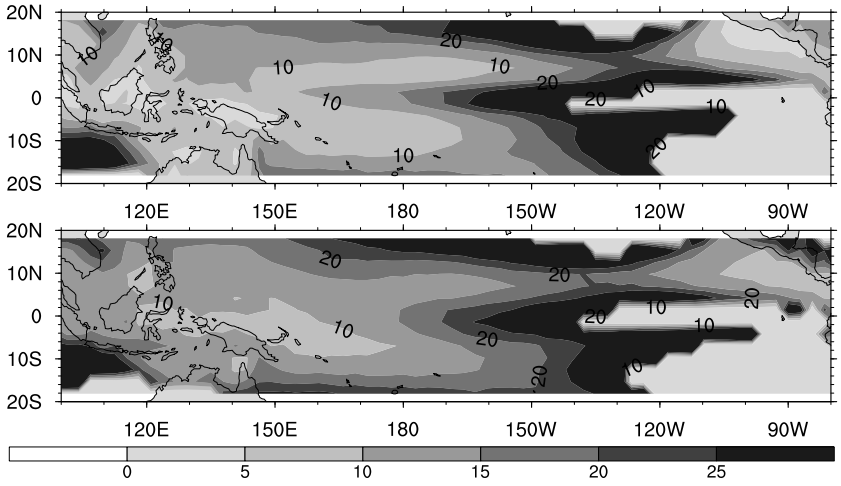

Fig. 3. Distribution of the fraction of annual mean stratiform precipitation (in percentage) in the control run (top) and in the SENS1 experiment (bottom). Areas with less than 0.6 m yr^{-1} annual average rainfall were not included.

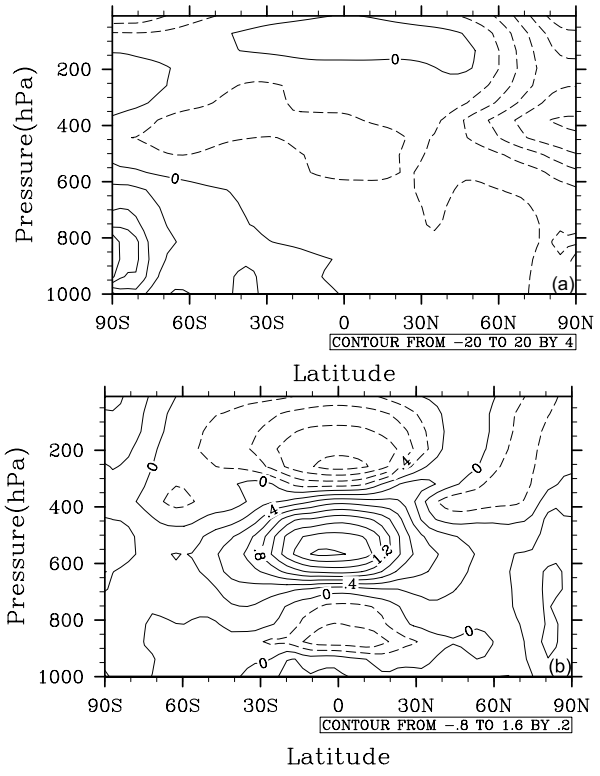

Fig. 4. The zonal mean temperature differences (K) between (a) the control run and the NCEP/DOE Reanalysis and between (b) the SENS1 and CNTRL.

stratiform precipitation is important for simulating the tropical intraseasonal oscillation (Liu et al., 2005). Wang et al. (2006) recently showed that increasing the convective entrainment/detrainment rate for shallow convection increases the fraction of stratiform precipitation in the deep tropics. Since, we have increased the convective entrainment/detrainment rate for shallow convection in our modified Tiedtke scheme, it is expected that the fraction of stratiform precipitation in the SENS1 experiment should be increased in comparison to that of the CNTRL. This is indeed true as shown in Fig. 3, where the spatial distribution of the fractions of 19-year mean stratiform precipitation in the total precipitation from the tropical region, as simulated are presented for both the CNTRL and SENS1 runs, respectively. As expected, the fraction of stratiform precipitation is greatly increased in the deep tropics in SENS1, consistent with the findings of Wang et al. (2006). On average, the fraction of stratiform precipitation was increased from 13% to 16% in the CNTRL and SENS1 experiments, respectively, between 20°S and 20°N, an increase of approximately 20%–30%.

Figure 4 shows the zonal mean temperature differences between the control run and the observations (a) and between the experiment SENS1 and the control run (b). Large differences between the control run and the observations occur mainly in the polar region (Fig. 4a). This could be due to the design of the dynamical core, which has a relatively coarse resolution in the latitudinal direction for a given even-area grid system within the polar region. In the control run, there are warm biases above the 300 hPa level and below the 700 hPa level, and a cold bias between the two levels in the middle and low latitudes (Fig. 4a). Although not totally eliminated, these biases are reduced to some degree in the experiment SENS1 (Fig. 4b), indicating that the modifications made to the convective scheme in SENS1 do improve the overall simulation of

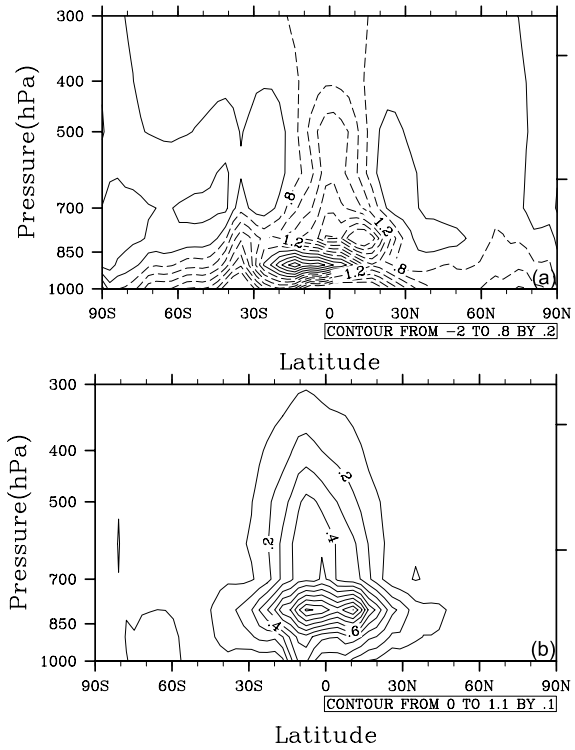

Fig. 5. As in Fig. 4 but for zonal mean specific humidity (g kg^{-1}).

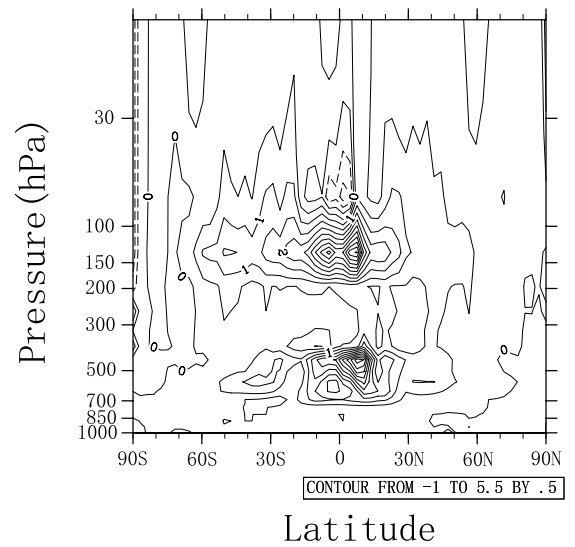

Fig. 6. The annual zonal mean cloud fraction differences between SENS1 experiment and the control run.

the mean vertical structure of the atmosphere.

The zonal mean specific humidity differences between the control run and the observations and between SENS1 and CNTRL are shown in Figs. 5a and b, respectively. In the control run, there is a small positive bias in specific humidity in the mid-high latitudes, significant dry biases near the surface and between 850 hPa and 600 hPa and a modest moist bias between 850 and 950 hPa in the low latitudes and in the lower troposphere within the Southern Hemisphere subtropics in comparison to the observations. With modifications to convection scheme in SENS1, the specific humidity in the tropical and subtropical regions is increased throughout the troposphere compared to CNTRL. In particular, a large increase between 700 hPa and 950 hPa in specific humidity in SENS1 compared to the CNTRL eliminates the dry bias in the tropics in the same layer that appeared in the CNTRL. The relatively moister troposphere in the SENS1 experiment in comparison to that obtained in the control run is consistent with the overall weaker/stronger convective/stratiform precipitation in SENS1 (Fig. 3) as the precipitating convection plays a role in drying the large-scale environment. The higher specific humidity in the SENS1 experiment also produces higher annual mean cloudiness, especially for the boundary layer clouds in the tropical and subtropical regions as well as high clouds in the deep tropics (Fig. 6). The increase in the boundary layer clouds are mainly a result of the suppressed shallow convection by the increased lateral entrainment/detrainment rate for such convection in the SENS1 experiment (Wang et al., 2004c). Furthermore, the global mean energy budget at the surface and the top of the model atmosphere was reduced by 0.4928 and 0.509 W m^{-2}, respectively, in SENS1 compared to CNTRL. However, the global mean energy imbalance of both the surface and the model top is significant in CNTRL, about -13 W m^{-2}.

3.2 *Interannual variability*

In addition to the mean climate discussed above, we also examined the interannual variability in the two simulations. To further study the effect on precipitation due to our modifications to the Tiedtke scheme, the spatial distributions of the temporal (19 years) standard deviation of precipitation is presented in figure 7 after removing the mean annual cycle from the observations, the CNTRL and the SENS1 runs. In general, the spatial distribution of the interannual variability is similar to that of the 19-year mean precipitation: regions with high precipitation have large interannual variability, such as over the western Pacific warm pool and the ITCZ regions. These features were reasonably simulated via both the CNTRL and SENS1 experiments although the models produced variability slightly stronger than that observed in the South Asian and Australian monsoon regions and in the coastal regions over the tropical eastern Pacific. Unfortunately, the variations over Antarctic could not be reproduced,

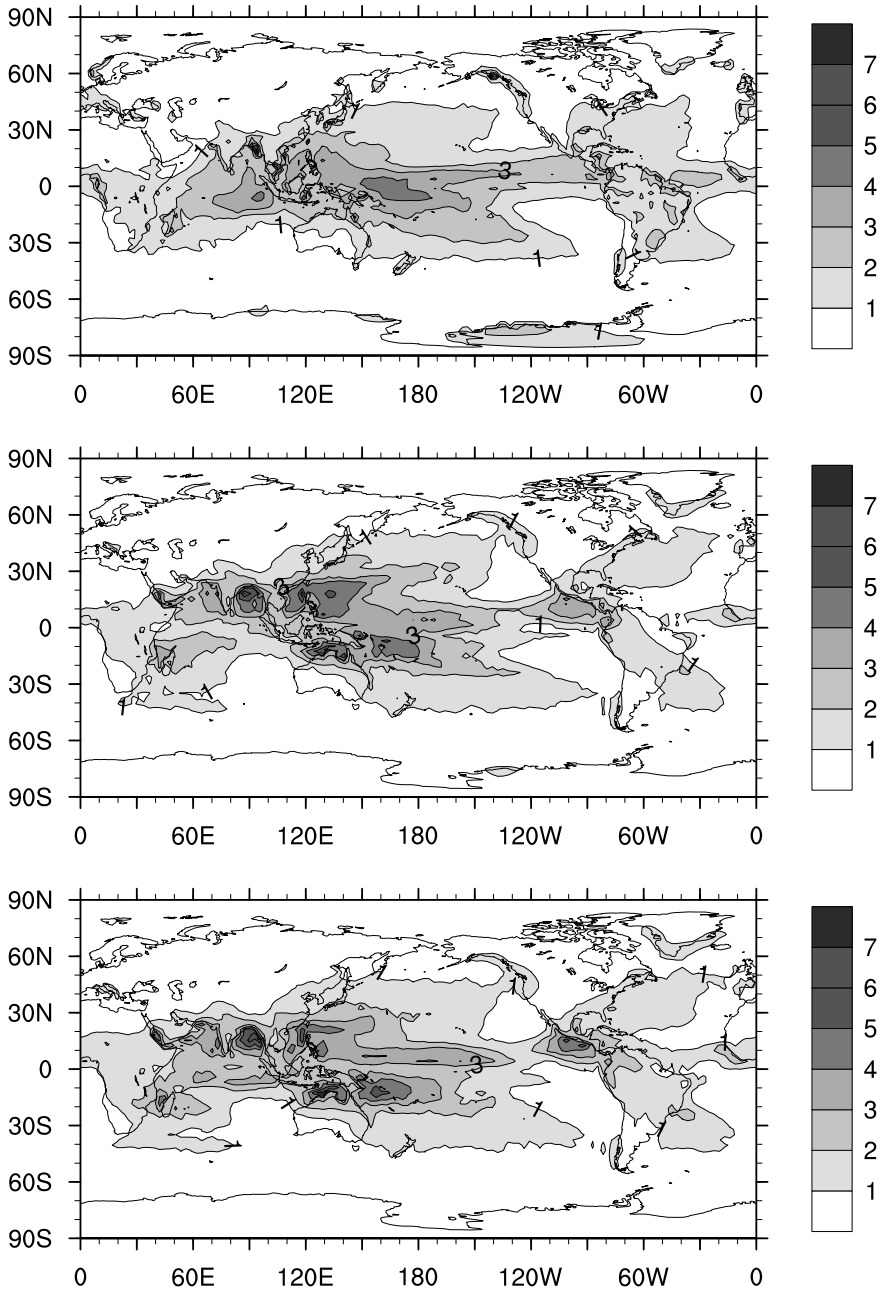

Fig. 7. The spatial distribution of the temporal standard deviation of the precipitation from the observations (top), from the SENS1 experiment (middle) and the CNTRL (bottom). Unit: mm d^{-1}.

probably due to the coarse resolution in the polar region, in both experiments. Both produced weaker interannual variability over the tropical South Indian Ocean and in the central-eastern Pacific ITCZ north of the equator. The global average, temporal, standard deviation after removing the mean annual cycle was 0.99 mm d^{-1}, 1.06 mm d^{-1} and 1.10 mm d^{-1} for the observation, SENS1 and control runs, respectively. It appears that overall the modifications to the Tiedtke convection scheme also reduce the bias in the simulated interannual variability of precipitation in GAMIL.

3.3 *Effects of individual changes*

As we have shown in the above discussion, our modifications to the Tiedtke convection scheme have led to significant improvements in the model simulation of the climatological mean state, especially in the

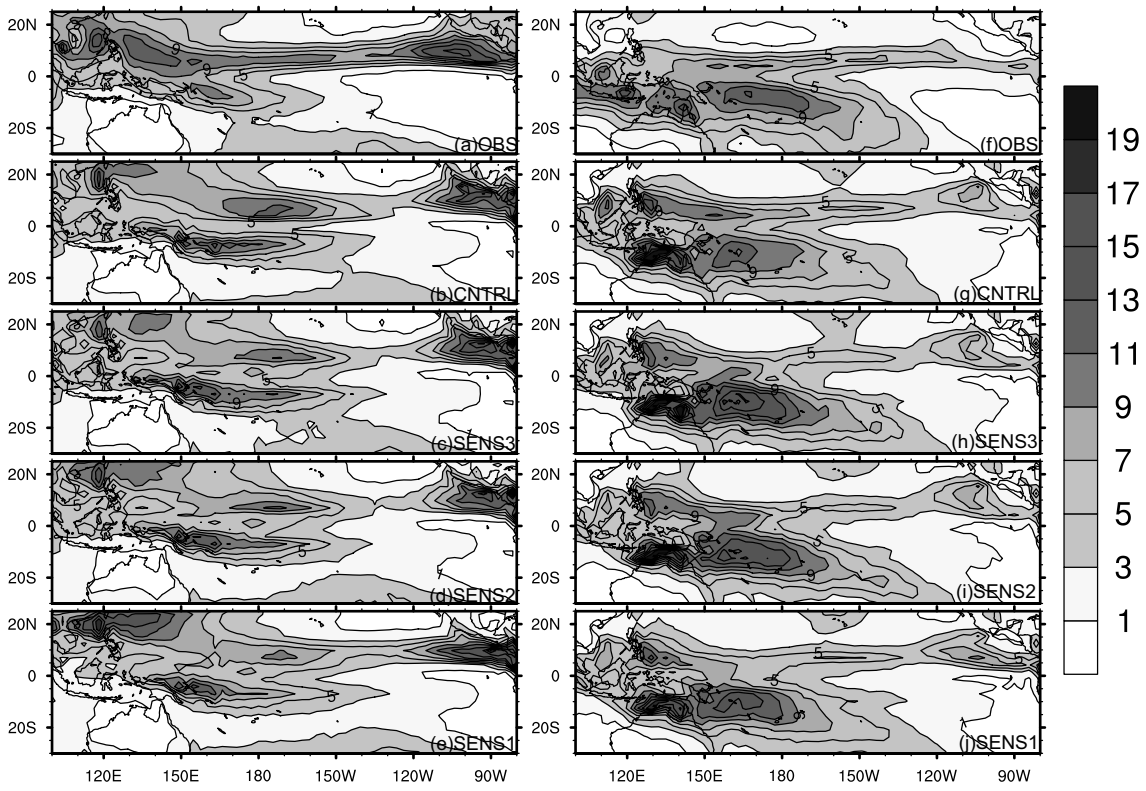

Fig. 8. The long-term mean boreal summer (left panel) and winter (right panel) precipitation in the tropical Pacific from Xie-Arkin, simulation of CNTRL, SENS3, SENS2, and SENS1. Unit: mm d^{-1}.

tropics, such as precipitation, temperature, specific humidity, and the interannual variability. Since three changes were made (see Table 1 and section 2.1), it would be interesting to examine which modification was most effective in leading to the improved simulations. We have performed several experiments (see Table 1) and found that the relative humidity threshold and the suppression of shallow convection were more influencial than the third modification. Therefore the results from the experiment without the relative humidity threshold (SENS2, Table 1) and with the suppressed shallow convection (SENS3, Table 1) are compared with experiments SENS1 and CNTRL, respectively, in this section. However, the contribution by the modification to the autoconversion coefficient in deep convection parameterization can be inferred from the difference between experiment SENS2 and SENS3. Note that since the major improvements are found in the tropical Pacific, our comparison will thus focus on this region.

Figure 8 shows the boreal summer (JJA) and winter (DJF) precipitation in the tropical Pacific from both the observations and the CNTRL, SENS3, SENS2, and SENS1 simulations, respectively. The differences between the experimental sensitivity are presented in Fig. 9. From Table 1, we can see that the difference between the experiment SENS3 and the control run represents the effect of the suppressed shallow convection on the improvements. Similarly, the differences between SENS2 and SENS3 and between SENS1 and SENS2 indicate the effects of the autoconversion coefficient change and RH threshold in deep convection, respectively.

In boreal summer, the "double ITCZ" precipitation over the western Pacific is significantly reduced in both the SENS2 and SENS3 experiments (Figs. 8c, d, and 9a, b) when compared to the control run (Fig. 8b), similar to the results observed for the SENS1 run (Figs. 8e). However, the precipitation in the central-eastern Pacific ITCZ in either SENS2 or SENS3 is similar to that observed in the control run, while it was greatly increased in SENS1 (Figs. 8e and 9c). Furthermore, the difference between the SENS2 and SENS3 experiments is very marginal (Fig. 9b), indicating that the modifications to the autoconversion coefficient in deep convection has little contribution to the improved simulation in either eliminating the "double ITCZ" problem or removing the gap in the ITCZ precipitation over the central-eastern Pacific. Note that the major difference between SENS2 and SENS1 occurs in the central-eastern Pacific and the western North Pacific (Figs. 8d, e, and 9c), with

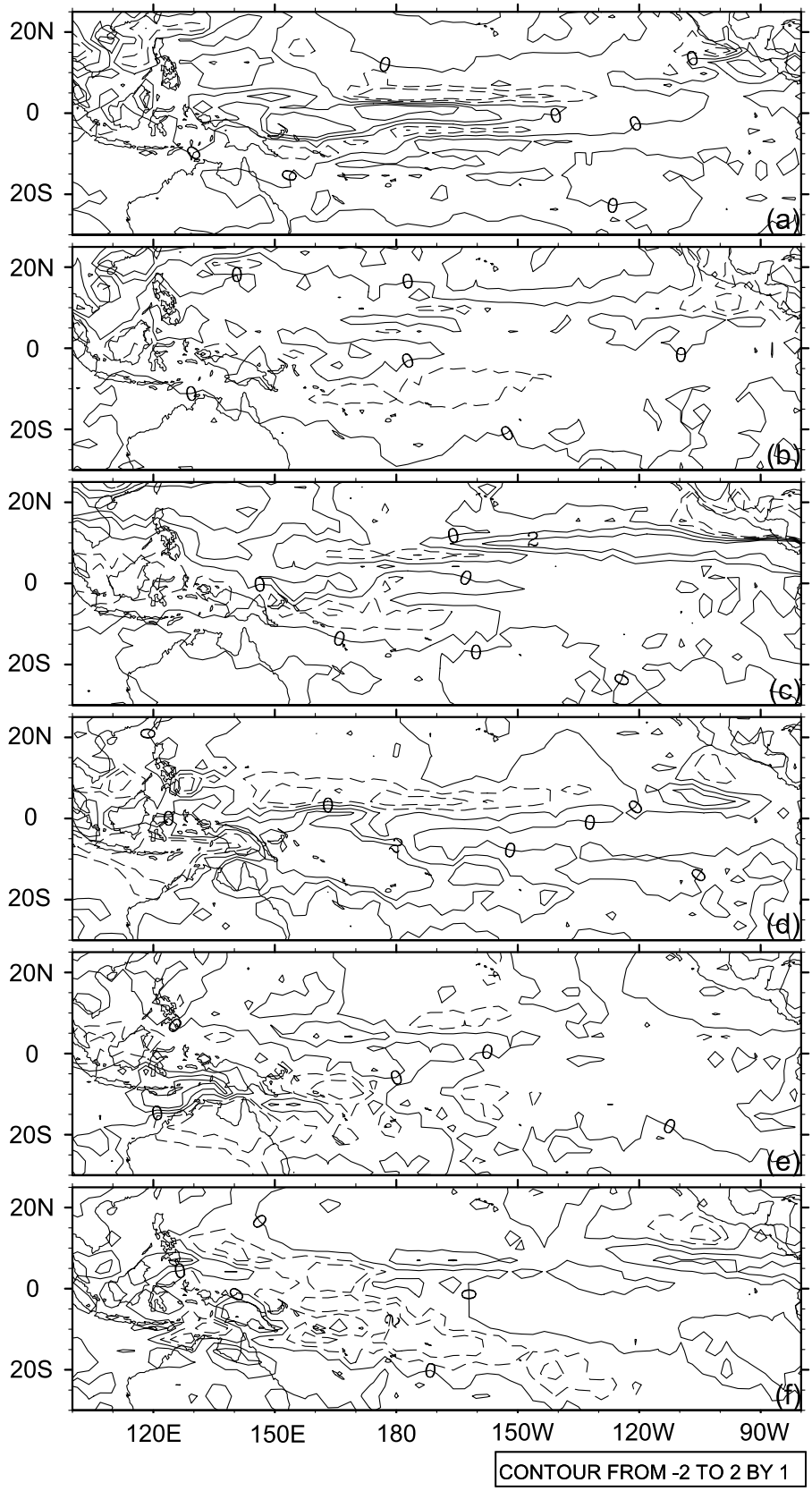

Fig. 9. The difference of long-term mean summer and winter precipitation in the tropical Pacific between experiments SENS3 and CNRTL (a, d), SENS2 and SENS3 (b, e), and SENS1 and SENS2 (c, f). Unit: mm d^{-1}.

the simulation from SENS1 being more realistic when compared with the observations (Fig. 8a). This indicates that the relative humidity threshold for deep convection triggering improves the model performance mainly over the northwestern and central-eastern Pacific. The improvement in the simulation of ITCZ precipitation in the western Pacific is mainly due to the modifications to the convective entrainment/detrainment for shallow convection in boreal summer within the model.

In boreal winter, the over estimation of the ITCZ precipitation from the western Pacific to north of the equator, is largely reduced in both SENS2 and SENS3 (Figs. 8h, i, and 9d) when compared to the CNTRL (Fig. 8g), which was reduced further in the SENS1 run (Fig. 8j), which provided the closest approximation of the observations (Fig. 8f). The precipitation in the SPCZ and the western Pacific ITCZ south of the equator was increased significantly in both SENS2 and SENS3, although they were overly estimated in comparison to the results from SENS1 (Fig. 8j). Therefore, SENS1 was more realistic when compared to the control run (Fig. 8f). Since the only difference between experiments SENS3 and CNTRL was the inclusion of the suppressed shallow convection in the former, the increase in precipitation south of the equator in SENS3 can thus be attributed to this modification in the Tiedtke scheme. This is consistent with the findings of Wang et al. (2005), and supported by the studies of McCaa and Bretherton (2004), von Salzen et al. (2005), and R. A. Neggers and his collaborators[c], who all found that suppression of the shallow convection would increase the subtropical marine boundary layer clouds on the winter hemisphere while increasing the ITCZ precipitation on the summer hemisphere. Similar to boreal summer, the differences between the results from SENS2 and SENS3 are again quite small (Fig. 9e), indicating that the modifications to the autoconversion coefficient in deep convection also do not contribute to the improved simulations in boreal winter. Furthermore, the inclusion of the RH threshold in deep convection triggering within the SENS1 experiment led to reductions in the precipitation over the western Pacific and in the SPCZ compared to SENS2 where the RH threshold was excluded. These results indicate that the significant improvement in the central-eastern and northwestern Pacific via the SENS1 simulations mainly result from the relative humidity threshold imposed on deep convection triggering, while the improvements in the "double ITCZ" region were mostly due to the suppressed shallow convection.

4. Summary

The grid-point atmospheric model (GAMIL) has been developed in the IAP LASG. The model uses a new dynamical core which solves the governing equations in a hybrid longitude/latitude grid system on the sphere and the model physics package is adopted from NCAR CAM2. When the model uses the Tiedtke mass-flux scheme to parameterize the subgrid scale convective processes, the model suffers from several severe deficiencies in the simulated precipitation in the tropics, such as the double ITCZ in the central-western Pacific, a break in ITCZ precipitation in the eastern Pacific in boreal summer, an underestimation in the SPCZ and an overestimation of the precipitation over South America and South Africa in boreal winter, although it does show its ability in simulating the global climate as a whole. These biases seem to result mainly from the treatment of subgrid scale convection in the model.

In order to reduce the systematic biases, we have introduced several modifications to the Tiedtke scheme used in GAMIL, including (1) an increase in lateral convective entrainment/detrainment rate for shallow convection, (2) inclusion of a relative humidity threshold for the triggering of deep convection, and (3) a reduced efficiency for the conversion of cloud water to rainwater in the convection scheme. The improvements in the simulation due to these modifications were evaluated with four experiments, each run for 20 years from 1 January 1979 to 31 December 1998, with the current climate settings as defined in the standard AMIP II experiments. The results show that both the climatological mean state and interannual variability in the model simulations are improved with the use of the modified scheme. In particular, the "double ITCZ" is eliminated and the break of ITCZ precipitation is removed in boreal summer, precipitation is increased in the SPCZ in boreal winter and is reduced over the South America and South Africa, and thus provides results that are more realistic. The modified scheme also considerably reduces both the cold and dry biases in the middle troposphere and increases the fraction of large-scale precipitation in the tropics. Results from several additional experiments show that the improvements in the northwestern and central-eastern Pacific mainly result from the introduction of the relative humidity threshold for the triggering of deep convection, while in the western Pacific is mainly due to the suppression of shallow convection.

Although the results from this study are encouraging, future studies are required to investigate the

[c]Neggers, R. A. J., J. D. Neelin, and B. Stevens, 2006: Impact mechanisms of shallow cumulus convection on tropical climate dynamics. *J. Climate,* (submitted).

sources of model bias in the high latitudes and to understand the effect of complex interactions among different physical processes within the model. For example, it is not clear how the modifications to the cumulus convective parameterization affect the boundary layer processes, and the model simulations. Furthermore, the radiation budget at the top of the model is required to be balanced, so as to avoid the drift in long-term integration. To this point, we have only examined the improvements in the simulated climate mean and interannual variability due to the modifications to the Tiedtke convective scheme, therefore, questions remain pertaining to improvements the modifications produced within the simulated annual cycle and intraseasonal variability in the tropics. These topics will be examined in a future study using the daily model output.

Acknowledgements. The authors thank Dr. Ping Liu and Prof. Bin Wang of the University of Hawaii for providing the codes of the Tiedtke convective scheme for GAMIL. The NCEP/DOE Reanalysis 2 and CMAP data used in this paper are provided by the NOAA-CIRES Climate Diagnostics Center, Boulder, Colorado, USA, from their web site at http://www.cdc.noaa.gov and the integration is performed on the Lenovo DeepComp 6800 Supercomputer at the Supercomputing Center of the Chinese Academy of Sciences. This work is jointly supported by CAS International Partnership Creative Group "The Climate System Model Development and Application Studies", the 973 Project (Grant No. 2005CB321703) and the Fund for Innovative Research Groups (Grant No. 40221503) and the National Natural Science Foundation of China (Grant No. 40233031).

REFERENCES

Collins，W. D., and Coauthors, 2003：Description of the NCAR Community Atmosphere Model (CAM2). National Center For Atmospheric Research, Boulder, Colo., 171pp.

Dümenil, L., and H.-S. Bauer, 1998: The tropical easterly jet in a hierarchy of general circulation models and the reanalyses. *MPI Report*, 243, 43pp.

Kanamitsu, M., and Coauthors, 2002: NCEP-DOE AMIP-II Reanalysis (R-2). *Bull. Amer. Meteor. Soc.*, **83**, 1631–1643.

Liu, P., B. Wang, K. Sperber, and J. Meehl, 2005: MJO in the NCAR CAM2 with the Tiedtke convection scheme. *J. Climate*, **18**, 3007–3020.

McCaa, J. R., and C. S. Bretherton, 2004: A new parameterization for shallow cumulus convection and its application to Marine subtropical cloud-topped boundary layers. Part II: Regional simulations of marine boundary layer clouds. *Mon. Wea. Rev.,* **132**, 883–896.

Mechoso, C. R., and Coauthors, 1995: The seasonal cycle over the tropical Pacific in coupled ocean-atmosphere general circulation models. *Mon. Wea. Rev.,* **123**, 2825–2838.

Nordeng, T. E., 1994: Extended versions of the convective parameterization scheme at ECMWF and their impact on the mean and transient activity of the model in the Tropics. ECMWF Tech. Memo. 206, 41pp.

Phillips, T. J., 1996: Documentation of the AMIP models on the World Wide Web. *Bull. Amer. Meteor. Soc.*, **77**, 1191–1196.

Roeckner, E., and Coauthors, 1996: The atmospheric general circulation model ECHAM-4: Model description and simulation of present-day climate. Max Planck Institute for Meteorology Rept. 218, 90pp.

Siebesma, A. P., and A. A. M. Holtslag, 1996: Model impacts of entrainment and detrainment rates in shallow cumulus convection. *J. Atmos. Sci.*, **53**, 2354–2364.

Tiedtke, M., 1989: A comprehensive mass flux scheme for cumulus parameterization in large-scale models. *Mon. Wea. Rev.*, **117**, 779–1800.

von Salzen, K., N. A. McFarlane, and M. Lazare, 2005: The role of shallow convection in the water and energy cycles of the atmosphere. *Climate Dyn.*, **25**, 671–688.

Wang Bin, and Coauthors，2004a: Design of a new dynamical core for global atmospheric models based on some efficient numerical methods. *Science in China* (*Ser A*), **47**, 4–21.

Wang, Y., O. L. Sen, and B. Wang, 2003: A highly resolved regional climate model (IPRC–RegCM) and its simulation of the 1998 severe precipitation event over China. Part I: Model description and verification of simulation. *J. Climate*, **16**, 1721–1738.

Wang, Y., S.-P. Xie, H. Xu, and B. Wang, 2004b: Regional model simulations of marine boundary layer clouds over the Southeast Pacific off South America. Part I: Control experiment. *Mon. Wea. Rev.*, **132**, 274–296.

Wang, Y., H. Xu, and S.-P. Xie, 2004c: Regional model simulations of marine boundary layer clouds over the Southeast Pacific off South America. Part II: Sensitivity experiments. *Mon. Wea. Rev.*, **132**, 2650–2668.

Wang, Y., S.-P. Xie, B. Wang, and H. Xu, 2005: Large-scale atmospheric forcing by Southeast Pacific boundary-layer clouds: A regional model study. *J. Climate*, **18**, 934–951.

Wang, Y., L. Zhou, and K. P. Hamilton, 2007: Effect of convective entrainment/detrainment on simulation of tropical precipitation diurnal cycle. *Mon. Wea. Rev.*, **135**(2), 567–585.

Xie, P., and P. A. Arkin, 1997: Global precipitation: A 17-year monthly analysis based on gauge observation, satellite estimates, and numerical model outputs. *Bull. Amer. Meteor. Soc.*, **78**, 2539–2558

Yu Rucong, 1994: a two-step shape-preserving advection scheme. *Adv. Atmos. Sci.*, **11**, 79–90.

Zhang, G. J., and N. A. McFarlane, 1995: Sensitivity of

climate simulations to the parameterization of cumulus convection in the Canadian Climate Centre general circulation model. *Atmosphere-Ocean*, **33**, 407–446.

Zhang, G. J., and N. A. McFarlane, 1995: Sensitivity of climate simulations to the parameterization of cumulus convection in the Canadian Climate Centre general circulation model, *Atmosphere-Ocean*, **33**, 407–446.

Zhang, G. J., and H. Wang, 2006: Toward mitigating the double ITCZ problem in NCAR CCSM3. *Geophys. Res. Lett.*, **33**, L06709, doi:10.1029/2005GL025229.